Available online at www.sciencedirect.com
ScienceDirect
Archives of Biochemistry and Biophysics 471 (2008) 207–214
ABB
www.elsevier.com/locate/yabbi

# Comparative study of catalase-peroxidases (KatGs)

Rahul Singh [1], Ben Wiseman, Taweewat Deemagarn, Vikash Jha, Jacek Switala, Peter C. Loewen *

*Department of Microbiology, University of Manitoba, Winnipeg, MB, Canada R3T 2N2*

Received 28 November 2007, and in revised form 14 December 2007
Available online 23 December 2007

**Abstract**

Catalase-peroxidases or KatGs from seven different organisms, including *Archaeoglobus fulgidus, Bacillus stearothermophilus*, *Burkholderia pseudomallei*, *Escherichia coli*, *Mycobacterium tuberculosis*, *Rhodobacter capsulatus* and *Synechocystis* PCC 6803, have been characterized to provide a comparative picture of their respective properties. Collectively, the enzymes exhibit similar turnover rates with the catalase and peroxidase reactions varying between 4900 and 15,900 $s^{-1}$ and 8–25 $s^{-1}$, respectively. The seven enzymes also exhibited similar pH optima for the peroxidase (4.25–5.0) and catalase reactions (5.75), and high sensitivity to azide and cyanide with $IC_{50}$ values of 0.2–20 μM and 50–170 μM, respectively. The $K_M$s of the enzymes for $H_2O_2$ in the catalase reaction were relatively invariant between 3 and 5 mM at pH 7.0, but increased to values ranging from 20 to 225 mM at pH 5, consistent with protonation of the distal histidine (pKa approximately 6.2) interfering with $H_2O_2$ binding to Cpd I. The catalatic $k_{cat}$ was 2- to 3-fold higher at pH 5 compared to pH 7, consistent with the uptake of a proton being involved in the reduction of Cpd I. The turnover rates for the INH lyase and isonicotinoyl-NAD synthase reactions, responsible for the activation of isoniazid as an anti-tubercular drug, were also similar across the seven enzymes, but considerably slower, at 0.5 and 0.002 $s^{-1}$, respectively. Only the NADH oxidase reaction varied more widely between $10^{-4}$ and $10^{-2}$ $s^{-1}$ with the fastest rate being exhibited by the enzyme from *B. pseudomallei*.


*Keywords:* Catalase; Peroxidase; KatG; Enzyme kinetics; NADH oxidase; Isoniazid

Catalase-peroxidases, or KatGs, are multifunctional enzymes present in bacteria, archaebacteria and some fungi [1]. The first example of this enzyme, HPI or hydroperoxidase I of *Escherichia coli*, was originally characterized as a catalase with a broad spectrum peroxidase activity (Fig. 1) giving rise to the name "catalase-peroxidase" [2]. Sequencing of the *katG* gene encoding HPI revealed the protein to have extensive similarity to plant peroxidases [3], and it was eventually categorized as a member of the Class I family of peroxidases [4]. However, whereas peroxidases are normally monomers, KatGs exist as homodimers or homotetramers of ~80 kDa subunits, each composed of two sequence related domains, possibly arising from a gene duplication and fusion event.

The crystal structures of KatGs from *Haloarcula marismortui* [5,6], *Burkholderia pseudomallei* [7,8], *Synechococcus* PCC 7942 [9], and *Mycobacterium. tuberculosis* [10] have been reported, and within their very similar peroxidase core structures, they all possess unique, catalase-specific, structural features not evident in peroxidases. The most striking of these features is the covalent cross-linking of the side chains of Met264, Tyr238 and Trp111 (numbering in *B. pseudomallei* KatG, BpKatG). In addition to these three residues, Arg426, which reversibly associates with Tyr238 to form a molecular switch modulating catalase activity [11,12], and Asp141 [13,14] are required for catalase activity but not peroxidase activity [15–20]. A perhydroxy modification of heme [8] and a pH dependent perhydroxy modifica-

* Corresponding author. Fax: +1 204 474 7603.
*E-mail address:* peter_loewen@umanitoba.ca (P.C. Loewen).
[1] Present address: Service de Bioénergétique, URA 2096 CNRS, Département de Biologie Joliot-Curie, CEA Saclay, 91191 Gif-sur-Yvette, France.

0003-9861/$ - see front matter © 2008 Elsevier Inc. All rights reserved.
doi:10.1016/j.abb.2007.12.008

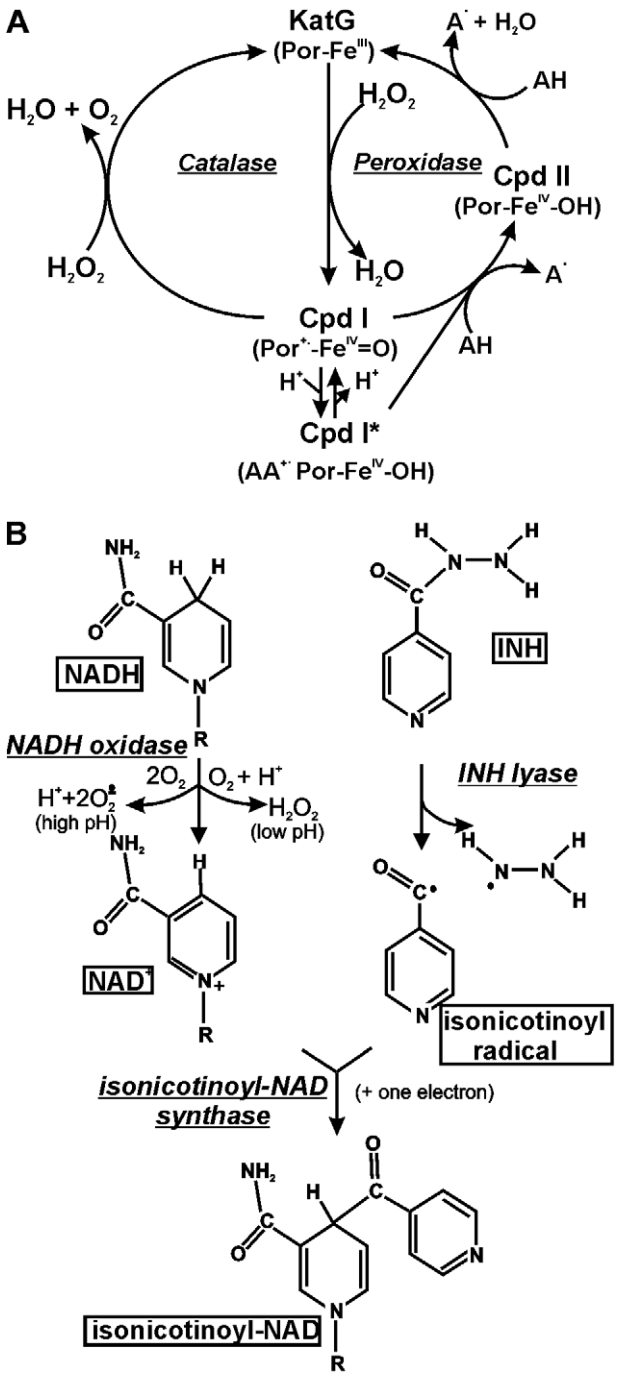


Fig. 1. Scheme outlining the various reactions catalyzed by KatGs.

tion of Trp111 [12,21] have also been reported in the structure of BpKatG, with the latter possibly having a role in NADH oxidase activity.

The wide spread interest in KatGs began with the observation that isoniazid resistance in *M. tuberculosis* was commonly associated with mutations in *katG* [22]. This was attributed to KatG activating isoniazid in a reaction that involves replacing the hydrazide portion of the molecule with an NAD moiety. The resulting activated form of isoniazid, isonicotinoyl-NAD, binds to InhA, an enoyl-acyl carrier protein reductase, inhibiting mycolic acid biosynthesis and, therefore, *M. tuberculosis* growth, [23,24]. The first step in the activation of isoniazid is removal of the hydrazine group (INH lyase in Fig. 1) [14,21,25], can occur independent of $NAD^+$ and $H_2O_2$, and is followed by coupling of the isonicotinoyl radical with $NAD^+$ (isonicotinoyl-NAD synthase in Fig. 1). The apparent complexity of the enzyme increased with the demonstration of a fifth enzymatic activity, that of an NADH oxidase (Fig. 1) which, from the standpoint of the INH activation reaction, confirmed that KatGs had a unique binding site for $NAD^+$ [14]. Surprisingly, despite this large number of reactions catalyzed by the protein, the actual in vivo role of the enzyme, aside from $H_2O_2$ removal, is unclear and the in vivo substrate for the peroxidase reaction remains unidentified.

The catalase and peroxidase reactions can be broken down into a number of stages. The formation of Compound I, classically a porphyrin cation radical, (reaction 1) is common to both the catalase and peroxidase reactions, but the subsequent reaction depends on the reducing substrate available. In the presence of high $H_2O_2$ concentrations, the catalase reaction proceeds (reaction 2), whereas at low $H_2O_2$ concentrations or if Cpd I is generated from an organic peroxide such as peroxyacetic acid, the longer life time of the intermediate allows electron dissociation from within the protein to quench the porphyrin radical. This generates radical sites on specific tyrosine and tryptophan residues and allows protonation of the oxoferryl group to form a hydroxoferryl heme (reaction 3). The name Cpd I* has come to be associated with this group of species which still lack two electron equivalents on the combined heme and protein compared to the native protein. One-electron transfers from peroxidase substrates reduce Cpd I* to an intermediate Cpd II and finally back to resting state (reactions 4 and 5).

$$\mathrm{Enz(Por-Fe^{III})} + \mathrm{H_2O_2} \rightarrow \mathrm{Cpd\ I(Por^{\cdot+}-Fe^{IV}=O)} + \mathrm{H_2O} \quad (1)$$

$$\mathrm{Cpd\ I(Por^{\cdot+}-Fe^{IV}=O)} + \mathrm{H_2O_2} \rightarrow \mathrm{Enz(Por-Fe^{III})} + \mathrm{O_2} + \mathrm{H_2O} \quad (2)$$

$$\mathrm{Cpd\ I(Por^{\cdot+}-Fe^{IV}=O)} \rightarrow \mathrm{Cpd\ I^{*}(Por-Fe^{IV}-OHTrp^{\cdot+})} \rightarrow \mathrm{Cpd\ I^{*}(Por-Fe^{IV}-OHTyr^{\cdot})} \quad (3)$$

$$\mathrm{Cpd\ I^{(*)}(Por^{\cdot+}/Trp^{\cdot}/Tyr^{\cdot}-Fe^{IV}-OH)} + \mathrm{AH} \rightarrow \mathrm{Cpd\ II(Por/Trp/Tyr-Fe^{IV}-OH)} + \mathrm{H^+} + \mathrm{A_{ox}} \quad (4)$$

$$\mathrm{Cpd\ II(Por/Trp/Tyr-Fe^{IV}-OH)} + \mathrm{AH} \rightarrow \mathrm{Enz(Por-Fe^{III})} + \mathrm{H_2O} + \mathrm{A_{ox}} \quad (5)$$

The NADH oxidation reaction requires molecular oxygen and produces either $H_2O_2$ (at pH <8.0, reaction 6) or $O_2^{\cdot-}$ (at pH >8.5, reaction 7) [14].

$$\mathrm{NADH} + \mathrm{O_2} + \mathrm{H^+} \rightarrow \mathrm{NAD^+} + \mathrm{H_2O_2} \quad (6)$$

$$\mathrm{NADH} + 2\mathrm{O_2} \rightarrow \mathrm{NAD^+} + 2\mathrm{O_2^{\cdot-}} + \mathrm{H^+} \quad (7)$$

A comparison of the kinetic properties of monofunctional catalases from 16 different sources revealed considerable diversity in reaction rates and inhibitor sensitivity despite the very similar core structures and sequences [26]. The catalase-peroxidases exhibit a similar uniformity of sequence and structure, but also a multiplicity of reactions, raising the question of whether there are significant variations in these different activities among the different KatGs. To answer this question, seven KatGs from six bacterial species, *Bacillus stearothermophilus* (BsKatG)[2], *B. pseudomallei* (BpKatG), *E. coli* (EcKatG), *M. tuberculosis* (MtKatG), *Rhodobacter capsulatus* (RcKatG), and *Synechocystis* PCC 6803 (SyKatG), and one archaebacterium, *Archaeoglobus fulgidus* (AfKatG) were selected for comparison of the kinetic parameters of the catalase, peroxidase, NADH oxidase, INH lyase and isonicotinoyl-NAD synthase activities.

## Materials and methods

### Strains and plasmids

The plasmids used in this work include pBpKatG [7] encoding BpKatG, pAH1 [25] encoding MtKatG, pBT22 [27] encoding EcKatG, pET3a [28] encoding SyKatG, perA [29] encoding BsKatG, pLUW640 [30] encoding AfKatG and pRcG-ET [31] encoding RcKatG. All of the plasmids were transformed into the catalase deficient *E. coli* strain UM262 (*pro leu rpsL hsdM hsdR endI lacY katE1 katG17*::Tn10 *recA*) [32] and grown in Luria broth containing 10 g/l tryptone, 5 g/l yeast extract, 5 g/l NaCl and 40 μg/l of hemin chloride for expression of the catalase-peroxidases. Subsequent purification of the enzymes was as described [7,8].

### Enzyme and protein determination

Catalase activity was determined by the method of Rørth and Jensen [33] in a Gilson oxygraph equipped with a Clark electrode. One unit of catalase is defined as the amount that decomposes 1 μmol of $H_2O_2$ in 1 min in a 60 mM $H_2O_2$ solution at pH 7.0 and 37 °C. Peroxidase activity was determined spectrophotometrically using ABTS (2,2′-azinobis(3-ethylbenzothiazolinesulfonic acid)) ($\varepsilon_{405} = 36{,}800\ M^{-1}\ cm^{-1}$) [34] or *o*-dianisidine ($\varepsilon_{460} = 11{,}300\ M^{-1}\ cm^{-1}$) [35] as electron donors. One unit of peroxidase is defined as the amount that decomposes 1 μmol of electron donor in 1 min in a solution of 0.4 mM ABTS or 0.36 mM *o*-dianisidine and 2.5 mM (for ABTS) or 1 mM (for *o*-dianisidine) $H_2O_2$ at pH 4.5 and 25 °C. INH lyase activity was followed by free radical production using nitroblue tetrazolium (NBT) reduction to a mono- and diformazan ($\varepsilon_{560} = 15{,}000\ M^{-1}\ cm^{-1}$ for monoformazan). NADH oxidase activity was determined spectrophotometrically at 340 nm using $\varepsilon = 6300\ M^{-1}\ cm^{-1}$ for NADH. Isonicotinoyl-NAD synthase activity was determined spectrophotometrically at 326 nm using $\varepsilon = 6900\ M^{-1}\ cm^{-1}$ for isonicotinoyl-NAD [36]. The protein was estimated according to the method of Layne [37]. Gel electrophoresis of purified proteins was carried out under denaturing conditions on 8% SDS–polyacrylamide gels [38,39].

[2] *Abbreviations used:* BsKatG, *Bacillus stearothermophilus* KatG; BpKatG, *B. pseudomallei* KatG; EcKatG, *E. coli* KatG; MtKatG, *M. tuberculosis* KatG; RcKatG, *Rhodobacter capsulatus* KatG; SyKatG, *Synechocystis* PCC 6803 KatG; AfKatG, *Archaeoglobus fulgidus* KatG; NBT, nitroblue tetrazolium; ABTS, 2,2′-azinobis 3-ethylbenzothiazolinesulfonic acid; CIP, *Coprinus cinereus* peroxidase.

## Results

### Purification

The KatGs were purified following a common protocol involving expression in a *katG* deficient mutant of *E. coli*, breaking the cells using a French press, treatment with streptomycin sulfate, precipitation with ammonium sulfate and ion exchange chromatography on DEAE-cellulose. Separation of the purified KatGs on a denaturing polyacrylamide gel reveals a predominant single band in each case suggestive of molecular weights ranging between 78 and 84 kDa (Fig. 2). A weaker band at approximately 160 kDa attributable to a small amount of cross-linked dimer not reduced by either β-mercaptoethanol or dithiothreitol is evident in EcKatG.

### Kinetic comparison of catalase and peroxidase activities

The comparison of kinetic data of the seven KatGs reveals relatively small variations in the catalase activities (2200–5400 U/mg, Table 1), and turnover rates (4900–15,800 $s^{-1}$, Table 2). It should be noted that occasional preparations of the enzymes exhibited activities that varied by up to 2-fold from those reported here [40] for reasons

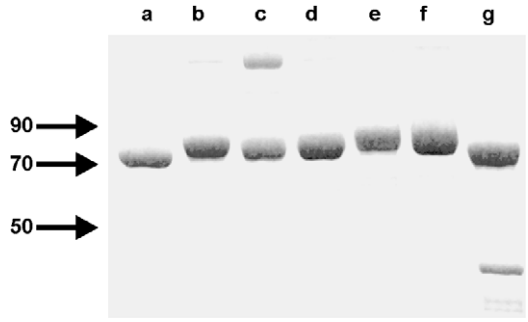


Fig. 2. SDS–polyacrylamide gel analysis of purified catalase-peroxidases. Samples were run on an 8% polyacrylamide gel. The locations and sizes (in kDa) of size markers are indicated by the arrows. The catalases in the various lanes are as follows: (lane a) BpKatG, (lane b) MtKatG, (lane c) EcKatG, (lane d) SyKatG, (lane e) BsKatG, (lane f) AfKatG and (lane g) RcKatG.

Table 1
Catalase and peroxidase specific activities of the various KatGs

| KatG | Catalase[a] | Peroxidase[b] | | pH[c] |
|---|---|---|---|---|
| | | ABTS | *o*-dianisidine | |
| AfKatG | 5280 ± 250 | 12.0 ± 3.3 | 3.2 ± 0.6 | 4.5 |
| BpKatG | 3630 ± 150 | 4.8 ± 0.9 | 5.3 ± 0.9 | 4.5 |
| BsKatG | 3120 ± 380 | 5.9 ± 1.6 | 5.3 ± 2.0 | 4.0 |
| EcKatG | 2200 ± 180 | 11.0 ± 1.3 | 8.3 ± 2.1 | 4.25 |
| MtKatG | 4450 ± 150 | 10.0 ± 2.5 | 8.8 ± 1.5 | 4.75 |
| RcKatG | 4830 ± 226 | 2.0 ± 0.3 | 1.0 ± 0.2 | 5.0 |
| SyKatG | 5420 ± 500 | 6.4 ± 2.1 | 5.5 ± 2.1 | 4.25 |

[a] U/mg = 1 μ mol $H_2O_2$ degraded per min per mg protein at pH 7.0.
[b] U/mg = 1 μ mol ABTS or *o*-dianisidine oxidized per min per mg protein.
[c] Optimum pH for peroxidase reaction.

Table 2
Kinetic parameters of the catalase reaction

| KatG | pH 7.0 | | | pH 5.5–6.0 | | |
|---|---|---|---|---|---|---|
| | $V_{max}$ [a] | $K_M$ [b] | $k_{cat}$ [c] | $V_{max}$ [a] | $K_M$ [b] | $k_{cat}$ [c] |
| AfKatG | 5500 ± 120 | 3.8 ± 0.3 | 7770 ± 170 | 11760 ± 220 | 32 ± 1.9 | 15680 ± 350 |
| BpKatG | 4300 ± 210 | 4.5 ± 0.9 | 5680 ± 280 | 11900 ± 280 | 56 ± 5.3 | 15900 ± 370 |
| BsKatG | 3410 ± 110 | 3.7 ± 0.7 | 4300 ± 150 | 5670 ± 150 | 90 ± 9.0 | 7600 ± 200 |
| EcKatG | 2220 ± 108 | 4.2 ± 0.8 | 2950 ± 140 | 3730 ± 50 | 35 ± 2.2 | 4970 ± 70 |
| MtKatG | 5700 ± 160 | 2.4 ± 0.5 | 4350 ± 210 | 7620 ± 400 | 225 ± 31 | 10200 ± 530 |
| RcKatG | 5100 ± 150 | 3.7 ± 0.9 | 6640 ± 190 | 10510 ± 240 | 30 ± 3.2 | 14100 ± 320 |
| SyKatG | 5400 ± 275 | 3.1 ± 0.7 | 7630 ± 380 | 6000 ± 80 | 20 ± 1.4 | 8000 ± 110 |

[a] $V_{max}$ (apparent), μ moles $H_2O_2$ $min^{-1}$ $mg^{-1}$.
[b] $K_M$ (apparent), [$H_2O_2$] at 0.5 $V_{max}$, mM.
[c] $k_{cat}$, $s^{-1}$.

that remain unclear. Thus, the variation in activity among the different KatGs is much smaller and the rates much slower than those exhibited by monofunctional catalases (54,000–833,000 $s^{-1}$). The first KatG characterized, EcKatG or HPI, was shown to be a broad substrate range peroxidase [2], and two peroxidase substrates with quite different structures were compared in this study, *o*-dianisidine (3,3′-dimethoxybenzidine) and ABTS (2,2′-azinobis(3-ethlybenzothiazolinesulfonic acid)). There is little difference between the reaction rates or pH optima with the two substrates by a single enzyme, but there is a 9-fold variation in the specific activities among the different enzymes which is greater than the variation in the catalase reaction rates (Table 1). In fact, the turnover rates for the peroxidase reactions vary over a smaller 3-fold range, (Table 3) and are significantly slower than for the catalase reaction falling in the range of 8–25 $s^{-1}$ consistent with the early observations that the catalase reaction of HPI predominated over the peroxidase reaction [2].

Like monofunctional catalases, the terms $V_{max}$, $k_{cat}$ and $K_M$ cannot be rigorously applied to the observed data because the two step catalase reaction does not follow a classical Michaelis–Menten pathway $E + S \leftrightharpoons E - S \rightarrow E + P$. Indeed, the data often do not fit the equation over the complete substrate range, particularly at higher concentrations where enzyme inhibition is evident. However, there is a close enough fit to the equation at lower substrate concentrations (Fig. 3) to allow the determination of "apparent" catalatic $V_{max}$, $K_M$ and $k_{cat}$ values (Table 2). The two step nature of the reaction is most evident in the very different apparent $K_M$ values for $H_2O_2$ in the peroxidase (60–1000 μM) and catalase (2.4–225 mM) reactions. The low $K_M$ in the peroxidase reaction reflects the higher affinity of the native enzyme for $H_2O_2$ in reaction 1 (heme oxidation to Cpd I) while the higher $K_M$ in the catalase reaction reflects the lower affinity for $H_2O_2$ by Cpd I in reaction 2 (Cpd I reduction by $H_2O_2$). Considerable variation in the apparent $K_M$ for the peroxidase substrate (7–300 μM ABTS, Table 3) is also evident among the enzymes indicating very different binding affinities among the enzymes.

Table 3
Kinetic parameters of the peroxidase reaction with ABTS

| KatG | $V_{max}$ [a] | $K_M$ [b] | $K_M$ [c] | $k_{cat}$ [d] |
|---|---|---|---|---|
| AfKatG | 12 ± 0.6 | 16 ± 4 | 95 ± 6 | 17 ± 0.8 |
| BpKatG | 6.0 ± 0.1 | 300 ± 21 | 700 ± 220 | 7.9 ± 0.1 |
| BsKatG | 8 ± 0.6 | 31 ± 8 | 210 ± 27 | 11 ± 0.8 |
| EcKatG | 18 ± 0.8 | 24 ± 5 | 60 ± 20 | 25 ± 1.1 |
| MtKatG | 14 ± 0.4 | 67 ± 7 | 360 ± 100 | 19 ± 0.5 |
| RcKatG | 5.9 ± 0.2 | 16 ± 1 | 830 ± 80 | 7.7 ± 0.3 |
| SyKatG | 9.3 ± 0.4 | 7 ± 1 | 1000 ± 60 | 13 ± 0.6 |

[a] $V_{max}$, μ mol ABTS $min^{-1}$ $mg^{-1}$.
[b] $K_M$, [ABTS] μM.
[c] $K_M$, [$H_2O_2$] μM.
[d] $k_{cat}$, $s^{-1}$.

The relatively narrow optimum pH ranges for the catalase and peroxidase reactions (Fig. 4A) using the standard assays were similar among the seven enzymes and consistent with previous reports [14,41–43], between pH 4 and 5 for peroxidase and between pH 6 and 6.5 for catalase (Fig. 4A). However, closer inspection of the data revealed that the $K_M$ for $H_2O_2$ in the catalase reaction was pH dependent (Fig. 4B) with the result that the 60 mM $H_2O_2$ used in the standard assay did not saturate all of the enzymes below pH 6.5. Using $H_2O_2$ concentrations up to 1000 mM to determine the apparent $k_{cat}$ and $K_M$ values over the complete pH range revealed a sharp, pH-dependent transition in the $K_M$ and changes in the $k_{cat}$ (Fig. 4B). In the case of BpKatG, the $K_M$ changed from the previously reported 5 mM at pH 7 to >60 mM above pH 6 with an inflection point for the transition at pH 6.2 (Fig. 4B). All six of the KatGs exhibited similar $K_M$s at pH 7 (2–5 mM) and similar inflection points for the change in $K_M$ as the pH was reduced. However, the different enzymes exhibited quite different $K_M$s below pH 6 with MtKatG exhibiting the highest $K_M$ at pH 5.0 (225 mM) and SyKatG the lowest (20 mM). Furthermore, the use of higher $H_2O_2$ concentrations revealed 2- to 3-fold faster turnover rates (Table 2) and optimum pH ranges that were broader and centered about a half pH unit lower at 5.5–5.75.

Monofunctional catalases, in particular the large subunit or clade 2 enzymes, exhibit exceptional thermal stability retaining activity even at temperatures above 80 °C. It was anticipated that the KatGs from the thermophiles *A. fugidus* and *B. stearothermophilus* might

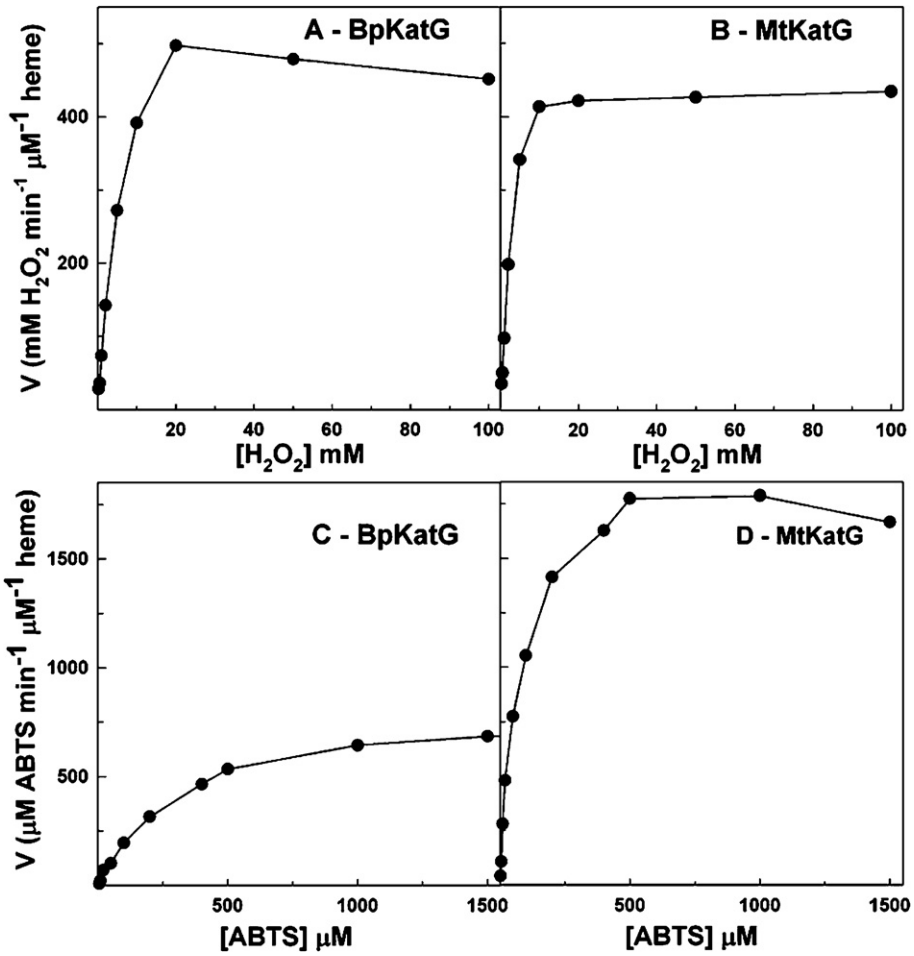


Fig. 3. Dependence of enzyme velocity on $H_2O_2$ concentration (catalase reaction in A and B) or ABTS concentration (peroxidase reaction in C and D). The representative enzymes included are BpKatG in A and C and MtKatG in B and D.

exhibit similar enhanced thermal stability as well, and this is indeed the case. Both AfKatG and BsKatG retained >80% of activity after 40 min of incubation at 65 °C. By comparison all of the other enzymes had lost all activity within 60–90 s (Table 4). Given the relatively similar sequences among the KatGs, a crystal structure of one of the two thermophilic enzymes is required to define the interactions that make those enzymes more resistant to denaturation.

KatGs are not sensitive to some of the common inhibitors of monofunctional catalases such as aminotriazole and thiol reagents. However, as expected of heme-containing enzymes, all of the KatGs exhibited sensitivity of catalase and peroxidase activities to cyanide and azide (Table 4). Both inhibitors were effective in the micromolar range with 50% inhibition occurring between 40 and 170 µM cyanide and 0.2–20 µM azide.

*Comparison of NADH oxidase and INH activation activities*

NADH oxidase activity in BpKatG was originally found to be significantly higher than in either MtKatG or EcKatG [14], and the additional four KatGs in this study, AfKatG, BsKatG, RcKatG and SyKatG all exhibit low oxidase levels (Table 5). Much higher cyanide and azide concentrations were required for inhibition of NADH oxidase with 10 mM cyanide and azide causing only 65% and 30% inhibition, respectively (data not shown), suggesting that the heme pocket is not the active center for the NADH reaction.

The INH lyase reaction, the first step in isoniazid activation, was investigated following formazan generation from the radical sensor NBT, with and without manganese ion in the reaction mixture. The rates of radical appearance in the presence of INH were similar for all KatGs with the exception of RcKatG which was 25% of the norm (Fig. 5 and Table 5). The addition of Mn enhanced radical production consistent with earlier reports that Mn enhances INH activation [44].

The key reaction in isoniazid activation is the joining of the isonicotinoyl radical from the INH lyase reaction with $NAD^+$ to form isonicotinoyl-NAD. A direct role for KatG as the catalyst in the ligation of isonicotinoyl radical and $NAD^+$ was initially questioned, but has subsequently been clearly documented [14,24,44]. The isonicotinoyl-NAD synthase activities of all the KatGs are similar, with

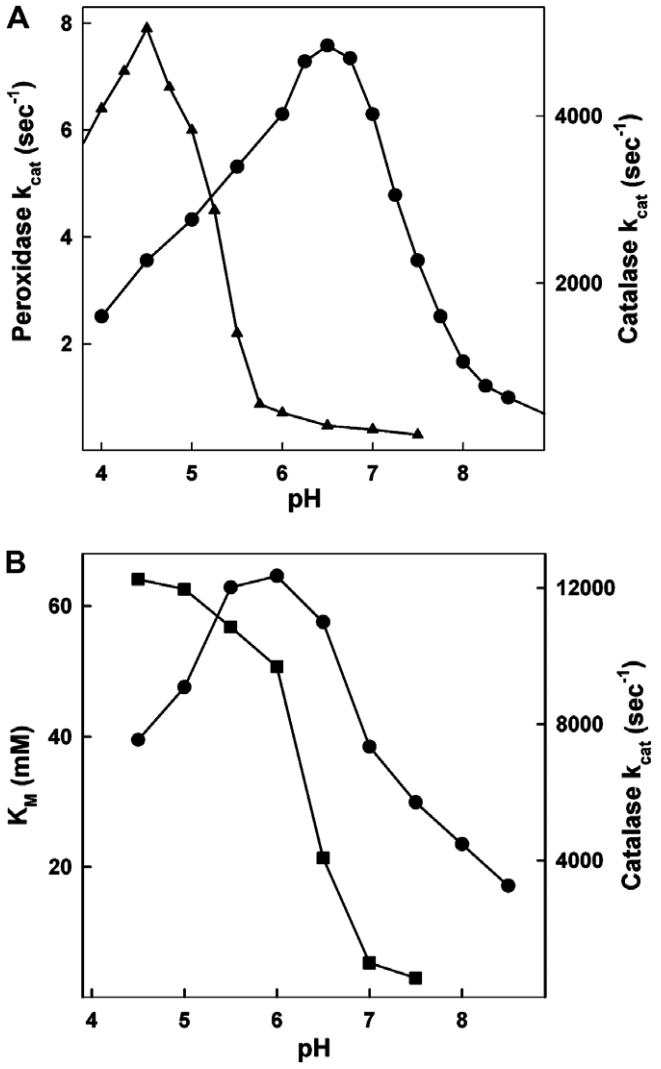


Fig. 4. (A) pH dependence of the turnover rates ($k_{cat}$) of the peroxidase (triangles) and catalase (circles) reactions of BpKatG determined under standard conditions (see text). (B) pH dependence of the $K_M$ (squares) and $k_{cat}$ (circles) of BpKatG.

Table 4
Time at 65 °C required for 100% inactivation and concentration of KCN and $NaN_3$ required for 50% inactivation of KatGs

| KatG | Time (min) at 65 °C | KCN, μM[a] (for 50% inactivation) | $NaN_3$, μM[a] (for 50% inactivation) |
|---|---|---|---|
| AfKatG | >40[b] | 150 | 20 |
| BpKatG | <1 | 40 | 8 |
| BsKatG | >40[c] | 50 | 2 |
| EcKatG | <1.5 | 50 | 7 |
| MtKatG | <1.5 | 100 | 0.2 |
| RcKatG | <1 | 80 | 8 |
| SyKatG | <1 | 170 | 13 |

[a] The enzyme was incubated with the inhibitor for 1 min before starting the reaction with $H_2O_2$.
[b] No inactivation was evident in 40 min.
[c] 20% inactivation was evident in 40 min.

that of BsKatG, followed closely by MtKatG, being the fastest and that of EcKatG being the slowest (Fig. 5 and Table 5).

Table 5
NADH oxidase, INH lyase and isonicotinoyl-NAD synthase activities

| KatG | NADH oxidase[a] | INH lyase[b] | | Isonicotinoyl-NAD synthase[c] |
|---|---|---|---|---|
| | | −Mn | +Mn | |
| AfKatG | 38 ± 6 | 7.0 ± 0.3 | 29.6 ± 0.4 | 0.15 |
| BpKatG | 510 ± 85 | 6.1 ± 0.2 | 32.8 ± 0.3 | 0.14 |
| BsKatG | 6 ± 6 | 5.0 ± 0.4 | 32.6 ± 0.3 | 0.19 |
| EcKatG | 15 ± 6 | 3.0 ± 0.2 | 35.2 ± 0.2 | 0.07 |
| MtKatG | 30 ± 3 | 6.2 ± 0.4 | 36.8 ± 0.8 | 0.17 |
| RcKatG | 30 ± 9 | 1.1 ± 0.2 | 21.6 ± 0.3 | 0.16 |
| SyKatG | 10 ± 3 | 4.6 ± 0.3 | 40.0 ± 0.5 | 0.16 |

[a] nmol NADH oxidized $min^{-1}$ μmol $heme^{-1}$ determined at 340 nm.
[b] μmol NBT reduced to monoformazan $min^{-1}$ $μmol^{-1}$ heme.
[c] μmol isnicotinoyl-NAD appearing $min^{-1}$ $μmol^{-1}$ heme.

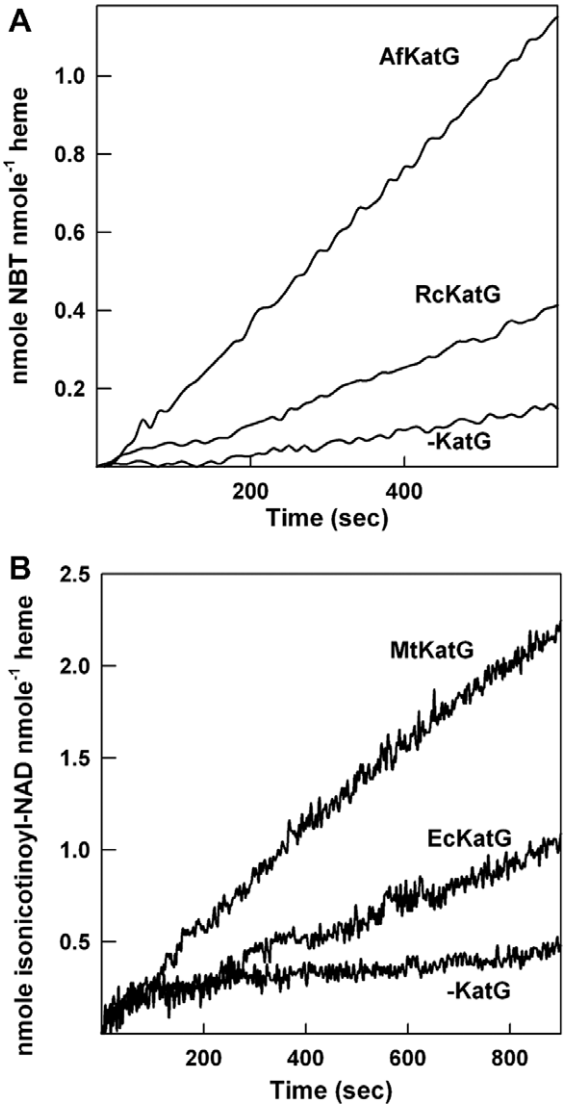


Fig. 5. Representative examples of the INH lyase reaction catalyzed by AfKatG and RcKatG (A) and of the isonicotinoyl-NAD synthase reaction catalyzed by MtKatG and EcKatG (B). The INH lyase reaction in (A) was followed by radical appearance monitored by NBT oxidation to formazan. The appearance of isonicotinoyl-NAD in (B) was monitored at 326 nm.

## Discussion

The catalase-peroxidases have a heme-containing active site that is highly conserved in both sequence and structure, and as a group, the seven KatGs studied present catalase, peroxidase, INH lyase and isonicotinoyl-NAD synthase activities that vary over a small 2- to 3-fold range. This is in contrast to sixteen heme-containing monofunctional catalases that presented catalase activities spread over a 10- to 20-fold range, despite their highly conserved sequences and structures [26]. Of the KatG-catalyzed reactions, only the NADH oxidase reaction presents significant variation over a 100-fold range among the enzymes studied.

A clear explanation for the broad range of activities among the monofunctional catalases has not emerged, although the architecture of the channels leading to the deeply buried heme, which vary in narrowness, length and contacting residues, is a likely determinant [45–47]. The main channel in KatGs is wider and relatively invariant in the four structures currently available, suggesting that $H_2O_2$ access should be relatively unimpeded in KatGs. Despite this, the turnover rate of the fastest KatG is 1/4 that of the slowest catalase and 1/50 that of the fastest. Therefore, while the catalatic turnover rate of KatGs is the fastest of its several reactions by at least 100 times, the active site of KatGs presents a far less optimal environment than that of monofunctional catalases for the catalase reaction. This is perhaps not surprising given the close structural relation of KatGs to plant peroxidases suggestive of the catalase reaction having been adapted to a peroxidase active site. The obvious catalase-specific residues added to the peroxidase core include the adduct of Trp111–Tyr238–Met264, a mobile Arg426, which associates with Tyr238, and Asp141, located in the entrance channel [48], but other residues outside of the narrow part of the main channel can also act as enhancers of the reaction. For example, the replacement of a Glu253 of SyKatG [41] and similar residues in BpKatG [unpublished data, TD and PL] cause a reduction in catalase activity to 25% of native levels. Whether these more distant residues control the entry of $H_2O_2$, modulate the actual electron transfer in the reduction reaction, or stabilize the solvent matrix in the channel leading into the active site remains to be determined. Whatever their role, it is clear that poorly understood, long distance effects are important in the catalase reaction in KatGs, and the challenge is to define their function.

The previously reported relatively sharp optimum pH range for the catalase reaction of KatGs, based on the standard assay conditions, has always been difficult to rationalize in terms of the functional groups involved. The more comprehensive review of the effect of pH on the catalatic $k_{cat}$ and $K_M$ for $H_2O_2$ (Fig. 4B and Table 2) shows that the optimum pH range is not as sharp as previously reported when higher $H_2O_2$ concentrations are used in the assays. The correlation between a decrease in substrate affinity and an increase in reaction rate was initially surprising, but it provides an important insight into the reaction pathway by implying two pH dependent processes. It was initially tempting to rationalize the change in affinity in terms of the pH sensitive transition of the mobile Arg426 between its R and Y conformations which has a midpoint at approximately pH 6.5 in the native enzyme [11,12]. However, the midpoint of the R to Y transition is shifted to much higher pH in Cpd I where there is 100% R conformation at pH 7.5 [12]. The other ionizable residue in the active site, the distal His112, is a more likely candidate, especially in light of the equivalent histidine in Cpd I of *Coprinus cinereus* peroxidase (CIP) exhibiting a pKa between 6 and 7, compared to 5 in the native state [49]. In other words, the decreased affinity of KatG for $H_2O_2$ at lower pH can be correlated with the increasing protonation of His112, which reduces the affinity for $H_2O_2$, most likely by interfering with hydrogen bond formation with $H_2O_2$ (Fig. 6). The inflection point of the $K_M$ profile suggests a pKa of 6.2 for His112 protonation, consistent with the data reported for CIP. The increase in reaction rate as pH drops, while seemingly at odds with the effect of pH on $K_M$, suggests a second pH dependent step in the reaction pathway. The two-electron (hydride ion) transfer from $H_2O_2$ to the ferryl oxygen during the reduction of Cpd I requires a proton for completion, and this would be facilitated at lower pH (Fig. 6). Therefore, increasing proton concentration affects the reaction pathway by decreasing the affinity of Cpd I for the substrate, but also by enhancing the catalytic process.

The reactions of KatG that remove hydrazine from isoniazid and subsequently attach the isonicotinoyl radical to

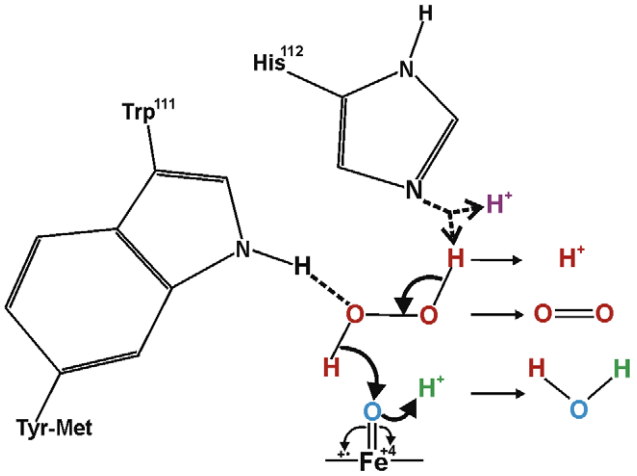


Fig. 6. Scheme illustrating how protons interfere with the binding of $H_2O_2$ to Cpd I of KatG, and facilitate the reduction of Cpd I. Increased $[H^+]$ causes protonation of His112 (proton shown in purple) which competes with hydrogen bond formation with $H_2O_2$ (shown in red) and makes $H_2O_2$ binding more difficult, consistent with the increase in $K_M$ at low pH. The transfer of two electrons to the ferryl oxygen from $H_2O_2$ for reduction of the oxoferryl porphyrin cation radical of Cpd I requires a proton (shown in green) for water generation. Higher $[H^+]$ will facilitate this part of the reaction, consistent with the faster turnover rate (higher $k_{cat}$) at lower pH. Trp111 is part of the M-Y-W (with Tyr238 and Met264) adduct found in all KatGs.

$NAD^+$ have not yet been associated with any other reactions of metabolic significance to the bacteria. Even in *M. tuberculosis*, it is clear that the two reactions are not an obvious benefit to the organism because they compromise growth through the activation of INH as an antitubercular drug. This observation coupled with the fact that all seven KatGs catalyze these reactions with similar rates suggests that they may be side reactions arising when isoniazid and $NAD^+$ bind at sites that have evolved for another reaction, most likely the peroxidase and oxidase reactions. The alternate possibility that the INH reactions are relics of a metabolic process or processes for which the demand has diminished is less likely because divergent evolution among the different bacteria in different environmental niches would be expected to give rise to greater variation in activities among different bacterial species. On the other hand, the greater variation in the NADH oxidase reaction may reflect it having presented a selective advantage, particularly in the environmental niche of *B. pseudomallei* which exhibits the highest activity.

## Acknowledgments

This work was supported by a Discovery Grant RGPIN 9600 from the Natural Sciences and Engineering Research Council of Canada (to P.C.L.) and by the Canada Research Chair Program (to P.C.L.).

## References

[1] M.G. Klotz, P.C. Loewen, Mol. Biol. Evol. 7 (2003) 1098–1112.
[2] W. Claiborne, I. Fridovich, J. Biol. Chem. 254 (1979) 4245–4252.
[3] B.L. Triggs-Raine, B.W. Doble, M.R. Mulvey, P.A. Sorby, P.C. Loewen, J. Bacteriol. 170 (1988) 4415–4419.
[4] K.G. Welinder, Curr. Opin. Struct. Biol. 2 (1992) 388–393.
[5] Y. Yamada, S. Saijo, T. Sato, N. Igarashi, H. Usui, T. Fujiwara, N. Tanaka, Acta Cryst. D57 (2001) 1157–1158.
[6] Y. Yamada, T. Fujiwara, T. Sato, N. Igarashi, N. Tanaka, Nat. Struct. Biol. 9 (2002) 691–695.
[7] X. Carpena, J. Switala, S. Loprasert, S. Mongkolsuk, I. Fita, P.C. Loewen, Acta Cryst. D58 (2002) 2184–2186.
[8] X. Carpena, S. Loprasert, S. Mongkolsuk, J. Switala, P.C. Loewen, I. Fita, J. Mol. Biol. 327 (2003) 475–489.
[9] K. Wada, T. Tada, Y. Nakamura, T. Kinoshita, M. Tamoi, S. Sigeoka, K. Nishimura, Acta Cryst. D58 (2002) 157–159.
[10] T. Bertrand, N.A.J. Eady, J.N. Jones, J.M. Nagy, B. Jamart-Grégoire, E.L. Raven, K.A. Brown, J. Biol. Chem. 279 (2004) 38991–38999.
[11] X. Carpena, B. Wiseman, T. Deemagarn, R. Singh, J. Switala, A. Ivancich, I. Fita, P.C. Loewen, EMBO Rep. 6 (2005) 1156–1162.
[12] X. Carpena, B. Wiseman, T. Deemagarn, B. Herguedas, A. Ivancich, R. Singh, P.C. Loewen, I. Fita, Biochemistry 45 (2006) 5171–5179.
[13] C. Jakopitsch, M. Auer, G. Regelsberger, W. Jantschko, P.G. Furtmuller, F. Ruker, C. Obinger, Biochemistry 42 (2003) 5292–5300.
[14] R. Singh, B. Wiseman, T. Deemagarn, L.J. Donald, H.W. Duckworth, X. Carpena, I. Fita, P.C. Loewen, J. Biol. Chem. 279 (2004) 43098–43106.
[15] A. Hillar, B. Peters, R. Pauls, A. Loboda, H. Zhang, A.G. Mauk, P.C. Loewen, Biochemistry 39 (2000) 5868–5875.
[16] G. Regelsberger, C. Jakopitsch, F. Ruker, D. Krois, G.A. Peschek, C. Obinger, J. Biol. Chem. 275 (2000) 22854–22861.
[17] S. Yu, S. Girotto, X. Zhao, R.S. Magliozzo, J. Biol. Chem. 278 (2003) 44121–44127.
[18] C. Jakopitsch, M. Auer, A. Ivancich, F. Ruker, P.G. Furtmuller, C. Obinger, J. Biol. Chem. 278 (2003) 20185–20191.
[19] C. Jakopitsch, A. Ivancich, F. Schmuckenschlager, A. Wanasinghe, G. Pöltl, P. Furtmüller, F. Rüker, C. Obinger, J. Biol. Chem. 279 (2004) 46082–46095.
[20] C. Jakopitsch, M. Auer, G. Regelsberger, W. Jantschko, P.G. Furtmüller, F. Rüker, C. Obinger, Eur. J. Biochem. 270 (2003) 1006–1013.
[21] T. Deemagarn, X. Carpena, R. Singh, B. Wiseman, I. Fita, P.C. Loewen, J. Mol. Biol. 345 (2005) 21–28.
[22] Y. Zhang, B. Heym, B. Allen, D. Young, S. Cole, Nature 358 (1992) 591–593.
[23] D.A. Rozwarski, G.A. Grant, D.H.R. Barton, W.R. Jacobs, J.C. Sacchettini, Science 279 (1998) 98–102.
[24] B. Lei, C.J. Wei, S.C. Tu, J. Biol. Chem. 275 (2000) 2520–2526.
[25] A. Hillar, P.C. Loewen, Arch. Biochem. Biophys. 323 (1995) 438–446.
[26] J. Switala, P.C. Loewen, Arch. Biochem. Biophys. 401 (2002) 145–154.
[27] B.L. Triggs-Raine, P.C. Loewen, Gene. 52 (1987) 121–128.
[28] C. Jakopitsch, F. Rüker, G. Regelsberger, M. Dockal, G.A. Peschek, C. Obinger, Biol. Chem. 380 (1999) 1087–1096.
[29] S. Loprasert, S. Negoro, H. Okada, J. Bacteriol. 171 (1989) 4871–4875.
[30] S. Kengen, F.J. Bikker, W.R. Hagen, W.M. de Vos, J. van der Oost, Extremophiles 5 (2001) 323–332.
[31] H. Forkl, J. Vandekerckhove, G. Drews, M.H. Tadros, Eur. J. Biochem. 214 (1993) 251–258.
[32] P.C. Loewen, J. Switala, M. Smolenski, B.L. Triggs-Raine, Biochem. Cell Biol. 68 (1990) 1037–1044.
[33] M. Rørth, P.K. Jensen, Biochim. Biophys. Acta 139 (1967) 171–173.
[34] R.E. Childs, W.G. Bardsley, Biochem. J. 145 (1975) 93–103.
[35] K.M. Moller, P. Ottolenghi, C.R. Trav. Lab. Carlsberg. 35 (1966) 369–389.
[36] R. Rawat, A. Whitty, P.J. Tonge, Proc. Natl. Acad. Sci. USA 100 (2003) 13881–13886.
[37] E. Layne, Methods Enzymol. 3 (1957) 447–454.
[38] U.K. Laemmli, Nature 227 (1970) 680–685.
[39] K. Weber, J.R. Pringle, M. Osborn, Methods Enzymol. 26 (1972) 3–27.
[40] R. Singh, J. Switala, P.C. Loewen, A. Ivancich, J. Am. Chem. Soc. 129 (2007) 15954–15963.
[41] C. Jakopitsch, E. Droghetti, F. Schmuckenschlager, P.G. Furtmüller, G. Smulevich, C. Obinger, J. Biol. Chem. 280 (2005) 42411–42422.
[42] M. Engleder, G. Regelsberger, C. Jakopitsch, P.G. Furtmüller, F. Rüker, G.A. Peschek, C. Obinger, Biochimie 82 (2000) 211–219.
[43] C.L. Varnado, K.M. Hertwig, R. Thomas, J.K. Roberts, D.C. Goodwin, Arch. Biochem. Biophys. 421 (2004) 166–174.
[44] C.J. Wei, B. Lei, J.M. Musser, S.C. Tu, Antimicrob. Agents Chemother. 47 (2003) 670–675.
[45] P. Chelikani, X. Carpena, I. Fita, P.C. Loewen, J. Biol. Chem. 278 (2003) 31290–31296.
[46] P.C. Loewen, X. Carpena, C. Rovira, A. Ivancich, R. Perez-Luque, R. Haas, S. Odenbreit, P. Nicholls, I. Fita, Biochemistry 43 (2004) 3089–3103.
[47] P. Chelikani, L.J. Donald, H.W. Duckworth, P.C. Loewen, Biochemistry 42 (2003) 5729–5735.
[48] T. Deemagarn, B. Wiseman, X. Carpena, A. Ivancich, I. Fita, P.C. Loewen, Proteins 66 (2007) 219–228.
[49] A.K. Abelskov, A.T. Smith, C.B. Rasmussen, H.B. Dunford, K.G. Welinder, Biochemistry 36 (1997) 9453–9463.